

# Strain-induced submicrocrystalline grains developed in austenitic stainless steel under severe warm deformation

A. BELYAKOV†‡, T. SAKAI†§, H. MIURA† and R. KAIBYSHEV‡

† Department of Mechanical Engineering and Intelligent Systems, The University of Electro-Communications, Chofu, Tokyo 182-8585, Japan

‡ Institute for Metals Superplasticity Problems, Ufa 450001, Russia

## ABSTRACT

Strain-induced grain evolution in a 304 type austenitic stainless steel has been studied in multiple compression with the loading direction being changed in each pass. The tests were carried out to total strains above 6 at 873 K ( $0.5T_m$ ) at a strain rate of about  $10^{-3} \text{ s}^{-1}$ . Multiple deformation promotes the rapid formation of many mutually crossing subboundaries because various slip systems operate from pass to pass. The gradual rise in misorientations across dislocation subboundaries with increasing strain finally leads to the evolution of very fine grains with large-angle boundaries. It is concluded that a new grained structure can result from a kind of continuous reaction during deformation, namely continuous dynamic recrystallization. Such deformation-induced grains are characterized by relatively low densities of dislocations, and considerable lattice curvatures developed in their interiors. The latter observations suggest that high elastic distortions are developed in the grain interiors and so such strain-induced grain structures are in a non-equilibrium state.

## § 1. INTRODUCTION

The properties of metals and alloys are strongly affected by their microstructures and, in particular, by the grain size. Very-fine-grained metallic materials have aroused considerable interest in materials science (Gleiter 1990). The development of fine-grained microstructures in sizeable samples is motivated by two main reasons: the improvement of workability and the control of mechanical properties for the products. Since grain refinement can be achieved by plastic deformation and annealing, studies of fine-grain evolution under thermomechanical processing conditions are of specific practical importance with high commercial potential.

The evolution of new grains during deformation is generally associated with dynamic recrystallization (DRX) (McQueen and Jonas 1975, Sakai and Jonas 1984). It is known that the dynamic grain size depends sensitively on the deformation conditions. Considerable refinement of the microstructure due to DRX can be obtained by decreasing the deformation temperature (or increasing the strain rate). On the other hand, the strain required for DRX initiation and, in particular, for its full completion increases with decreasing temperature. This makes studies of large deformation at low temperatures difficult by conventional deformation methods. Recently, several specific techniques have been proposed to provide severe

plastic deformations (Armstrong *et al.* 1982, Valiev 1996, Humphreys *et al.* 1999). Armstrong *et al.* (1982) showed that the flow stresses approach a saturation value at very large accumulated strains, while the dislocation density in subgrain interiors decreases. The subboundaries are more sharply defined and some of them look like conventional grain boundaries at high strains. The mechanisms for structural evolution at high strains have been the subject of some debate; however, it is generally believed that new grain evolution results from a kind of continuous reaction on the substructural level (Valiev *et al.* 1996, Iwahashi *et al.* 1997, Belyakov *et al.* 1998). It should also be noted that fine-grained materials produced by severe deformation are characterized by high internal stresses, which may be associated with the non-equilibrium state of the strain-induced grain boundaries (Furukawa *et al.* 1998, Belyakov *et al.* 2000). Detailed understanding of the nature of the residual stresses evolved in fine-grained materials, however, is complicated by a scarcity of adequate experimental data.

The aim of this work is to study the fine-grained microstructures developed in an austenitic stainless steel during severe warm deformation and, in particular, to analyse the elastic distortions that evolve in strain-induced submicron-scale grains.

## § 2. EXPERIMENTAL PROCEDURE

A 304 type austenitic stainless steel (0.058% C, 0.7% Si, 0.95% Mn, 0.029% P, 0.008% S, 8.35% Ni, 18.09% Cr, 0.15% Cu, 0.13% Mo and the balance Fe) with an initial grain size of about 25  $\mu\text{m}$  was used as the samples for multipass compressions with sequential rotation of the specimen from pass to pass. This type of deformation may be considered as a kind of multiple forging. The samples were machined into a rectangular shape with starting dimensions of 9.8 mm : 8.0 mm : 6.5 mm. This dimensional ratio of about 1.5 : 1.22 : 1.0 did not change during multiple compression while the loading direction was changed through 90° from pass to pass (i.e.  $x$  to  $y$  to  $z$  to  $x$ ...), when the maximal ratio (1.5) is changed to the minimal ratio (1.0) at each compression, that is  $\varepsilon = \ln(1.0/1.5) = -0.4$ . The tests were carried out in vacuum using boron nitride powder as a lubricant at 873 K ( $0.5T_m$ ) and a strain rate of about  $10^{-3} \text{ s}^{-1}$ . The deformed specimens were water quenched, ground to right-angle shapes, and then reheated to the test temperature. Microstructural analysis was carried out with a JEM-2000FX transmission electron microscope on sections parallel to the last compression axis. Misorientations of the strain-induced subboundaries were studied using the conventional Kikuchi-line technique. The small lattice curvatures that evolved in the new grain interiors were analysed using the component of the rotation vector lying in the plane of the electron diffraction pattern; this involved an accuracy of about 0.1°.

## § 3. EXPERIMENTAL RESULTS AND DISCUSSION

### 3.1. *Microstructure development under multiple-deformation conditions*

A series of stress-strain curves plotted for 16 consecutive compression passes is shown in figure 1. The general shape of the flow curve envelope is similar to that associated with dynamic recovery. Strain hardening is clearly evident at low strains below 1.0 and the differences between the yield stresses at reloading and the flow stresses immediately before unloading become quite small after the third compression, leading to steady-state-like behaviour for the overall flow curve. It may be concluded, therefore, that static recrystallization does not take place during

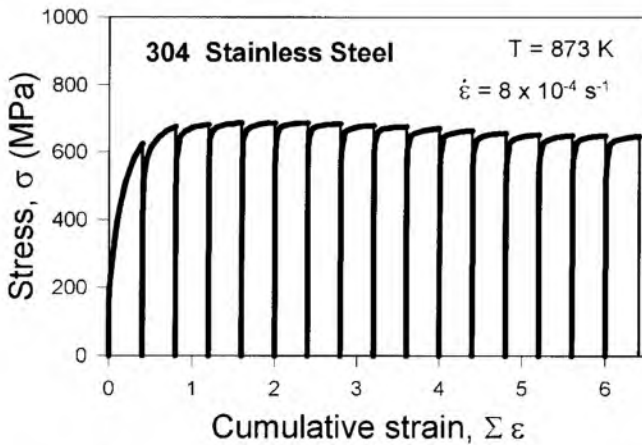


Figure 1. Stress-cumulative strain curves plotted over 16 compressions with a change of the loading direction in each pass.

reheating for the present multiple deformations at  $0.5T_m$ ; so the structural changes are mainly affected by strain accumulation and dynamic recovery.

Multiple deformation to a cumulative strain of 6.4 resulted in the evolution of a very-fine-grained structure with an average grain size of about  $0.3 \mu\text{m}$ . Figure 2 shows a typical micrograph of such a microstructure. It is clearly seen that the strain-induced fine grains are outlined by medium- to large-angle boundaries with average misorientations of about  $27^\circ$ . It should also be noted here that some fine grains contain only a few dislocations in their interiors. The structural changes

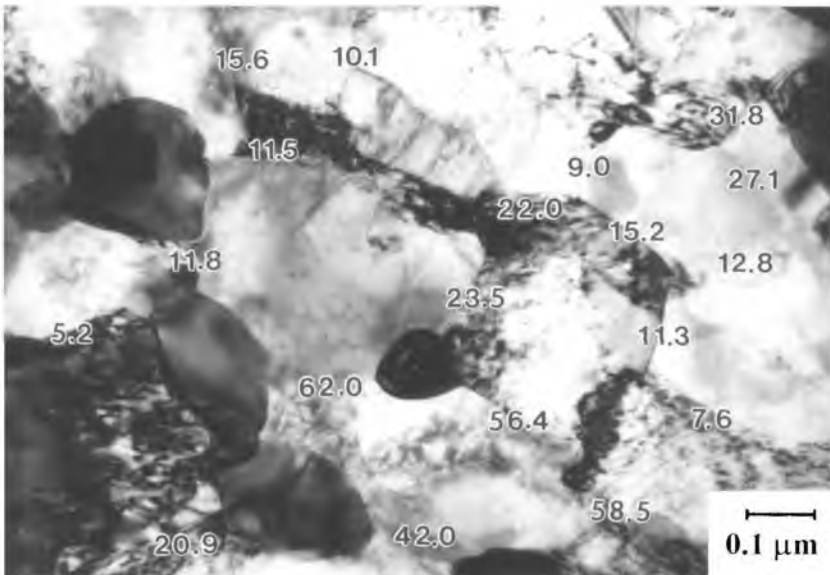


Figure 2. A typical fine-grained microstructure in the 304 stainless steel developed by multiple warm compressions to a total strain of 6.4. The numbers indicate the misorientations associated with the strain-induced boundaries in degrees.

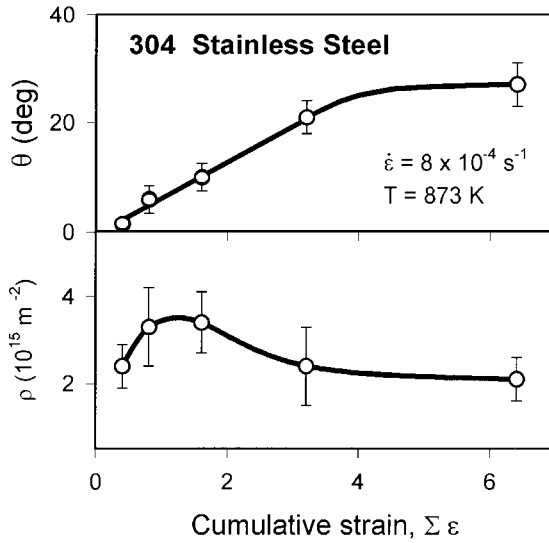


Figure 3. Effect of multiple warm deformations on the average misorientation  $\theta$  of strain-induced (sub)grains and the dislocation density  $\rho$  developed in their interiors.

leading to these new grains are illustrated in figure 3, which shows the variations in the average misorientation  $\theta$  between (sub)grains and in the dislocation densities  $\rho$  in their interiors with cumulative strain. It is clearly seen that strain accumulation results in increasing  $\theta$  up to values typical of conventional grain boundaries and, in contrast, in decreasing  $\rho$  following a rapid rise during early deformation. Both  $\theta$  and  $\rho$  approach constant values at strains above 3, where a new grained structure is fully developed (figure 2). It is concluded, therefore, that the development of such fine-grained microstructures can result from continuous evolution of the dislocation substructures caused by warm deformation. This is similar to continuous or rotation DRX (Humphreys and Hatherly 1996, Belyakov *et al.* 1999).

### 3.2. Internal stresses evolved in new grains

To study the internal stresses that evolve in strain-induced fine-grained structures, some of the dislocation-free grains were chosen for closer examination. Two typical examples of such grains are represented in figures 4(a) and (c). The letters in the grain interiors (i.e. A to D) indicate five local regions in a grain, within which the orientations of the crystal lattice were measured. The electron diffraction patterns obtained from the grains are plotted in figures 4(b) and (d) as fragments of Kikuchi maps. The lettered points indicate the positions on the central electron beam associated with each local region in figures 4(a) and (c). The lattice curvatures existing between the selected areas can be roughly evaluated by measuring distances between the points in the diffraction patterns. Misorientations corresponding to the lattice curvatures were calculated in the diffraction plane between each region and they ranged from  $0.2^\circ$  to  $0.7^\circ$ , as shown in figures 4(a) and (c).

The lattice curvatures of the fine grains in figures 4(a) and (c) may be more clearly illustrated by the bent surfaces in figures 5(a) and (b), respectively. Assuming, for simplicity, the areas outlined by A–B–C–D to be squares, the relative altitudes on the surfaces shown here were plotted from the deviations of the central

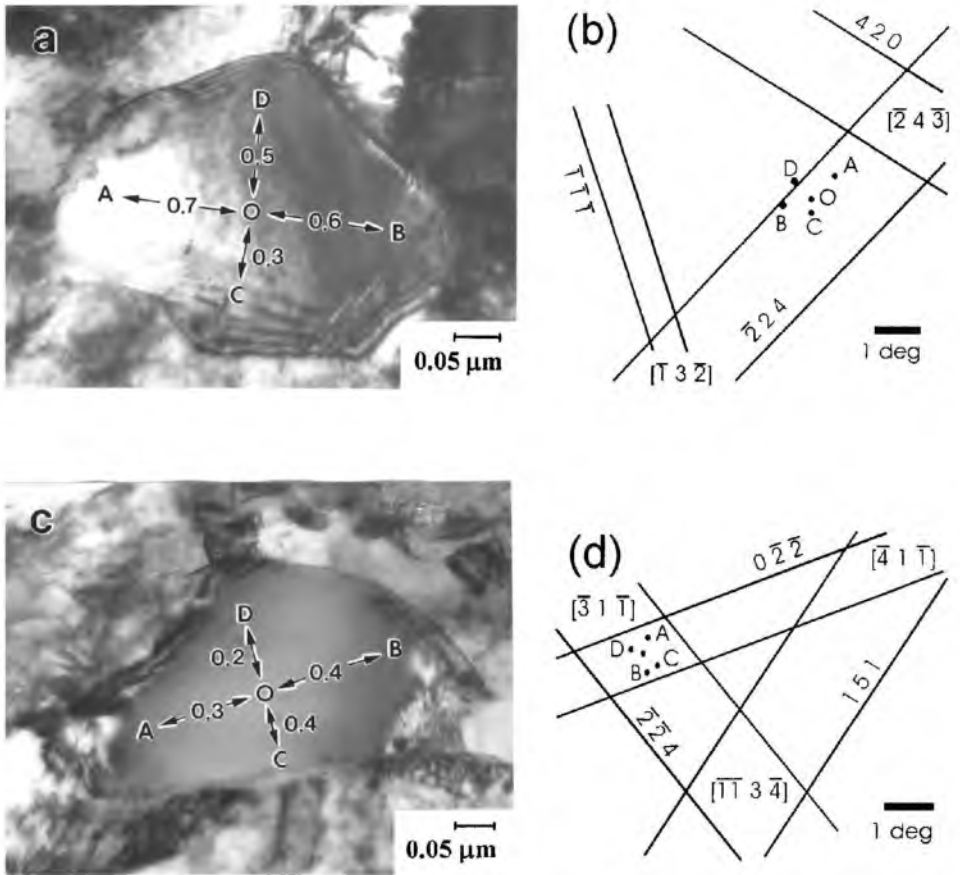


Figure 4. (a), (c) Typical dislocation-free fine grains evolved in 304 stainless steel by multiple warm deformations to a high cumulative strain of 6.4. The numbers in (a) and (c) indicate the lattice curvatures between the lettered points in degrees. (b), (d) Diffraction patterns as fragments of Kikuchi maps obtained from the grains in (a) and (c) respectively.

electron spots in the Kikuchi map from that for the grain centre (i.e. region O), the altitude of which was taken to be zero. These surfaces may be considered as a type of crystallographic plane perpendicular to the central beam, namely  $[2\bar{4}3]$  and  $[31\bar{1}]$  in figures 4(b) and (d) respectively. The relative altitudes are shown in units of  $10^{-3}d$ , where  $d$  is the distance between the diagonal points A–B and C–D. It is clearly seen in figure 5 that very complicated elastic distortions evolve in these strain-induced grains. The general feature of lattice bending developed in such grains is their saddle-shaped curvatures. It should also be noted that the lattice distortions in the grain interiors may change non-monotonically from place to place. This is suggested by detailed consideration of the altitude variations between some points, for instance A–C and D–B in figures 5(a) and (b), respectively.

The lattice curvatures that evolve in some dislocation-free grains were analysed quantitatively by measuring the misorientations between local regions separated by distances of about 0.1–0.15  $\mu\text{m}$ . The results are shown in figure 6. The most frequent values of elastic curvature lie in the range 0.2–0.3°, although they may reach 1.0° and

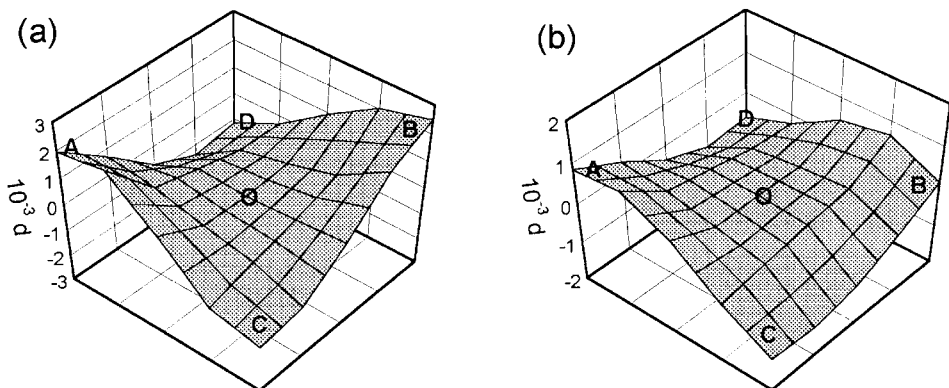


Figure 5. (a), (b) Three-dimensional representations of the bent lattice planes in the strain-induced grains in figures 4(a) and (c) respectively. The relative altitudes are shown in units of  $10^{-3}d$ , where  $d$  is the diagonal dimension of the square base, that is A-B and C-D.

the average value is about  $0.4^\circ$ . It should be noted here that the true lattice curvatures are higher than those presented in figure 6, because only one component of the rotation vector, that lying in the plane of the diffraction pattern, was analysed. Assuming that the elastic strain changes linearly with respect to the specimen thickness with a zero-point at half of the latter, the elastic normal strain  $\varepsilon$  and shear strain  $\gamma$  that evolve in the bent grains can be roughly evaluated as follows:  $\varepsilon = \Delta/d = t'\theta_\varepsilon/d$  and, similarly,  $\gamma = t'\theta_\gamma/d$ , where  $d$  is the distance between the measured points,  $t'$  is the distance from the midpoint of specimen thickness, and  $\theta_\varepsilon$  and  $\theta_\gamma$  are the rotation angles responsible for the normal and shear strains respectively. Then the maximal elastic strains are developed near the surfaces of the specimens, that is at  $t' = 0.5t$ , where  $t$  is the foil thickness (150–200 nm). The residual normal stresses  $\sigma$  and shear stresses  $\tau$  associated with the maximal value of the elastic distortions can be derived as  $\sigma/E = 0.5t\theta_\varepsilon/d$  and  $\tau/G = 0.5t\theta_\gamma/d$ , where  $E$  and  $G$  are Young's modulus and the shear modulus respectively at 873 K (Frost and Ashby 1982). The internal stresses corresponding to the lattice curvatures in figure 6 are represented in figure 7. The values of the normal and shear internal

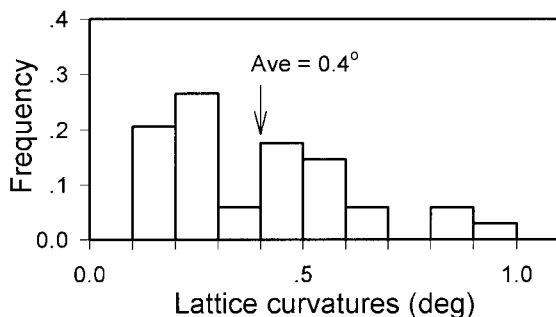


Figure 6. The lattice curvatures that evolve in the new fine grains during multiple deformations to a strain of 6.4 at 873 K. Note that here only the strain-induced fine grains that were almost free of dislocations were analysed.

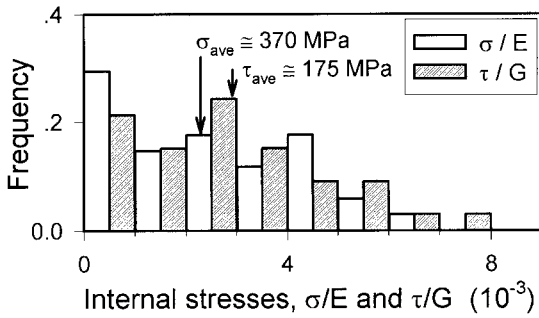


Figure 7. Internal normal elastic stress  $\sigma$  and shear elastic stresses  $\tau$  in the strain-induced fine grains after multiple deformation at 873 K. These were evaluated through the lattice distortions in figure 6. The  $\sigma$  and  $\tau$  values were normalized using Young's modulus and the shear modulus respectively.

stresses averaged over the all measured grains in figure 7 were evaluated to be about 370 and 175 MPa respectively. The former is over half the warm flow stress at high strains (see figure 1). The lack of dislocations in these fine grains can result from the high elastic distortions accumulated in the strain-induced grains that evolve through intensive plastic working.

The fine new grains developed at high strains result from the transformation of high-density subgrains with medium to high misorientations formed at low to moderate strains, as described above. Plastic deformation breaks up the initial grains into domains with different combinations of operative slip systems and leads to the evolution of geometrically necessary boundaries (GNBs) between different domains (Kuhlmann-Wilsdorf and Hansen 1991, Hughes and Hansen 1997). Multiple compressions with changes of loading direction can accelerate the evolution of mutually crossing GNBs owing to promotion of the variations in slip systems operating at each deformation pass. The misorientations of such dislocation subboundaries can increase rapidly with further deformation as a result of the accumulation of so-called grain boundary or misfit dislocations coming from different slip systems. It should be noted that under such conditions the excess dislocations are inhomogeneously distributed in these (sub)grain boundaries and cannot be fully relaxed because of the relatively low temperature of  $0.5T_m$ . It can be concluded, therefore, that the elastic lattice distortions are associated with the non-equilibrium state of the strain-induced grain-boundaries and that they remain stable in these fine grains. The high internal stresses can act as back stresses to dislocation movement. They may be responsible for both the decrease in dislocation density in the fine grain interiors and the hardening of materials subjected to severe deformation. It can be concluded, therefore, that the dislocation-free grains that appear at high strains result not only from dynamic recovery but also from the high internal stresses owing to their non-equilibrium states.

#### § 4. CONCLUSIONS

The very fine-grained microstructure that evolves in a 304 type stainless steel under conditions of large warm deformation was studied by the multiple compression of rectangular samples at 873 K ( $0.5T_m$ ) with changes in the loading direction. The main results can be summarized as follows:

- (1) New grains with a size of about 0.3  $\mu\text{m}$  develop at high cumulative strains above 6 as a result of the gradual increase in misorientation between dislocation subgrains caused by warm deformation.
- (2) These fine grains are characterized by a low internal density of dislocations and by saddle-shaped lattice curvatures. The latter suggest that complex elastic distortions and associated high internal stresses develop in the grain interiors.
- (3) It is concluded that such high internal stresses can be attributed to the strain-induced grain boundaries and their non-equilibrium states.

#### ACKNOWLEDGEMENTS

The authors are grateful for financial support from the Recrystallization and Texture Committee of the Iron and Steel Institute of Japan as well as to the NKK Co. Ltd, for supplying the test material. One of authors (A.B.) would also like to express his hearty thanks to the Inoue Foundation for Science and to the Japan Science and Technology Corporation for providing scientific fellowships. Useful discussions with Dr S. Dmitriev (The University of Electro-Communications, Tokyo) are also acknowledged with gratitude.

#### REFERENCES

- ARMSTRONG, P. E., HOCKETT, J. E., and SHERBY, O. D., 1982, *J. Mech. Phys. Solids*, **30**, 37.
- BELYAKOV, A., GAO, W., MIURA, H., and SAKAI, T., 1998, *Metall. Trans. A*, **29**, 2957.
- BELYAKOV, A., SAKAI, T., MIURA, H., and KAIBYSHEV, R., 1999, *Iron Steel Inst. Japan Int.*, **39**, 593; 2000, *Scripta mater.*, **42**, 319.
- FROST, H. J., and ASHBY, M. F., 1982, *Deformation-Mechanism Maps* (Oxford: Pergamon), p. 60.
- FURUKAWA, M., HORITA, Z., NEMOTO, M., VAKIEV, R., and LANGDON, T., 1998, *Phil. Mag. A*, **78**, 203.
- GLEITER, H., 1990, *Prog. Mater. Sci.*, **33**, 1.
- HUGHES, D. A., and HANSEN, N., 1997, *Acta Mater.*, **45**, 3871.
- HUMPHREYS, F. J., and HATHERLY, M., 1996, *Recrystallization and Related Annealing Phenomena* (Oxford: Pergamon), p. 380.
- HUMPHREYS, F. J., PRANGNELL, P. B., BOWEN, J. R., GHOLINIA, A., and HARRIS, C., 1999, *Phil. Trans. R. Soc. A*, **357**, 1663.
- IWAHASHI, Y., HORITA, Z., NEMOTO, M., and LANGDON, T. G., 1997, *Acta mater.*, **45**, 4733.
- KUHLMANN-WILSDORF, D., and HANSEN, N., 1991, *Scripta metall. mater.*, **25**, 1557.
- MCQUEEN, H. J., and JONAS, J. J., 1975, *Treatise Mater. Sci. Tech.*, **6**, 393.
- SAKAI, T., and JONAS, J. J., 1984, *Acta Metall.*, **32**, 189.
- VALIEV, R. Z., 1996, *Ann. Chim. Fr.*, **21**, 369.
- VAKIEV, R. Z., IVANISENKO, YU. V., RAUCH, E. F., and BAUDELET, B., 1996, *Acta mater.*, **44**, 4705.